Title: Complex network analysis of completely extended chains in rubber elasticity

Authors: Yoshifumi Amamoto[1,2,3]*, Ken Kojio[1], Atsushi Takahara[1], Yuichi Masubuchi[4], Mariko I. Ito[2], Takaaki Ohnishi[2]*

Affiliations:

[1]Institute for Materials Chemistry and Engineering, Kyushu University, 744 Motooka, Nishi-ku, Fukuoka 819-0395, JAPAN

[2]Graduate School of Artificial Intelligence and Science, Rikkyo University, 3-34-1 Nishi-Ikebukuro, Toshima-ku, Tokyo 171-8501, JAPAN

[3]Graduate School of Social Data Science, Hitotsubashi University, 2-1 Naka, Kunitachi, Tokyo 186-8601, JAPAN

[4]Graduate School of Engineering, Nagoya University, Furo-cho, Chikusa-ku, Nagoya 464-8603, JAPAN

Abstract: Rubber elastic theory describes the relationship between the microscopic chain structure and macroscopic mechanical properties of soft network polymers, such as elastomers and gels. When the deformation exceeds a certain threshold, the formation of extended chains induces hardening and failure of the materials, which has been tackled by experiments involving measurement techniques and mechanochemistry. However, the relationship between the network structure as concerns connectivity and the formation behavior of extended chains has hardly been described. Herein, we demonstrate the quantification of chain connectivity based on complex network science to investigate the formation mechanism of completely extended chains in rubber elasticity. Polymer chains in the central position of the network tended to persist in the extended chains as concerns connectivity. Furthermore, the formation of extended chains induces neighboring polymer chains to become extended chains, causing stress concentration at the network scale. Our approach, based on complex network theory, is useful as a bridge between conventional theory and experiments for describing complicated rubber elasticity at the mesoscale.

INTRODUCTION

Several attempts have been made to understand rubber elasticity through experimentation, theory, and simulation. The origins of elasticity can be classified into entropy and energy elasticity[1-3]. The former exhibits a unique behavior compared to other materials, where the conformation of the polymer chains determines the elasticity of the bulk materials. Therefore, explaining the mechanism of rubber elasticity based on the deformation of polymer chains along with that of bulk materials is important. In the initial stage, the neo-Hookean model is often considered, in which the end-to-end distances of the polymer chains obey a Gaussian distribution (Fig. 1a)[4]. As the elongations proceed, a deviation of the distances from the Gaussian distribution owing to finite chain extensibility causes an increase in stress, and the non-Gaussian chain theory is adopted (Fig. 1b)[1, 5-7]. Furthermore, extended or forced chains are formed (Fig. 1c)[8-16], and the dissociation of the chains results in macroscopic failure of the bulk materials[17-20].

The network structure of polymer chains in elastomers and gels significantly affects rubber elasticity[21-29]. The polymer chains in these materials are connected by cross-linking points to form networks. During the preparation of the materials used in the experiments, the fluctuation and/or distribution of the molecules always form a heterogeneous network, which affects the deformation behavior of the polymer chains. Quantification of the network structure is one of the key points for accessing heterogeneous networks in rubber elasticity[30-32]. Several studies on rubber elasticity have focused on network heterogeneity, such as dangling chains, loop chains, number of cross-linking points, and connectivity[21-29], which reflect the local network structure. Recently,

authors analyzed the heterogeneous structure of elastomers based on complex network science, an area in data science[32-34], which enables us to quantify the heterogeneity of networks from larger or global network scales[32, 35]. The closeness centrality reveals the role of each cross-linking point and polymer chain in rubber elasticity.

The theoretical treatment of an extended chain is often troublesome. The formation of extended chains is critical for rubber elasticity, as mentioned, and is closely related to several mechanical behaviors, such as strain hardening or failure of the materials[9-16]. The forces on the chain scales and strain crystallization were revealed by experimental approaches such as mechanochemistry and neutron scattering[36-39]. Furthermore, chain sessions and macroscopic failure have been reproduced in simulations considering dangling or loop chains[40-42]. However, only few examples describing this phenomenon quantitatively exist, because treating complicated network structures, such as connectivity and/or entanglement, is difficult. For instance, the difference between homogeneous and heterogeneous networks in the formation behavior of extended chains has not been clearly investigated. Furthermore, the formation mechanism and place where the extended chains are formed in the polymer network have hardly been evaluated. Another open question is whether the formation of an extended chain affects neighboring polymer chains.

In this study, we described the formation of a completely extended chain using a quantitative indicator of cross-linking points and/or polymer chains from the perspective of complex network science (Fig. 1). Closeness centrality, one of the indicators in complex network analysis, was utilized to analyze the mechanism and place

of formation of a completely extended chain in network heterogeneity. Furthermore, the stress concentration at the network scale was discussed using the assortativity coefficient, degree of cross-linking points, and length of clusters in the network comprising the extended chain.

RESULTS

Preparation and uniaxial elongation of elastomer

As a representative soft elastic material, elastomers were constructed and deformed using coarse-grained molecular dynamics simulations because the connectivity of elastomers cannot be quantitatively evaluated easily using experimental methods. The elastomers were prepared by crosslinking two complementarily reactive four-arm star polymers at the chain ends (Fig. 2), as previously reported[35]; in fact, they have been utilized in the synthesis of tetra-PEG gels[43, 44]. The polymers were crosslinked at several concentrations, i.e., $c/c^* = 3$, 1, and 0.3 (where c is the crosslinked concentration, and c^* is the overlap concentration of the star polymers) with high conversions and then reduced to the same density to obtain elastomers. Therefore, the crosslinking densities of the elastomers were almost identical, whereas the connectivity of the molecular chains among the crosslinking points was different. Subsequently, the elastomers were elongated uniaxially. The numbers of beads and bonds between crosslinking points were set as $N_{\mathrm{xlp\text{-}xlp}} = 22$ and $N_{\mathrm{bond}} = 23$, respectively, which resulted in less entanglement effects on the stresses due to the short chains (Figs. 3(a) and 3(b)). For a comparison, a diamond-like elastomer, where the crosslinked points and molecular chains were mimicked as carbon

and carbon–carbon bonds, respectively, was constructed and uniaxially elongated as a homogeneous elastomer. To discuss the neighbors of the extended chains, the number of crosslinking points or star polymers was set to 512 (= 8 × 8 × 8).

In the rubber elastic model, the upturn in stress-strain curve is closely related to a finite extensibility[8-16], where the molecular chain between crosslinking points is extended and aligned toward the elongated direction owing to the limit of the chain length (Fig. 1). The network structure dependence of the finite extensibility effect was confirmed via stress–strain curves, where the stress was normalized by the right side of a neo-Hookean model without considering the finite chain extensibility, as follows:

$$\sigma = G(\lambda^2 - \lambda^{-1}), \qquad (1)$$

where σ is the stress, G the shear modulus, and λ the elongation ratio (Fig. 4a). The value of G is obtained from the plateau regions of the plot and is almost identical to the theoretical values of the phantom network models ($G = \nu k_B T(1 - \frac{1}{f})$; ν: crosslinking density; f: branch number) at $c/c^* = 1$, as previously reported[35]. As the crosslinking concentrations increased, the regions that deviated from the horizon line at 1 appeared in the earlier stage of elongation. This is attributable to the finite chain extensibility because the neo-Hookean model does not consider this effect. The diamond-like network deviated from the phantom network model at λ = 4–5, which is consistent with the theory that the model is valid at $\lambda < (Nr_0)^{0.5} \approx 4.8$, where N and r_0 are the number of bonds and the equilibrium bond length, respectively[4]. Additionally, when the stress–strain curves were fitted using an elastic model with consideration of the non-Gaussian chain, the parameter

$\alpha \sim \lambda_{max}^{-1}$, where λ_{max} is the maximum extensibility[22], depended significantly on the crosslinking concentrations, although the number of bonds was set as $N_{bond} = 23$ (Fig. 3c). This indicates that the elongation ratio where the stress deviated from the neo-Hookean model depended on the cross-linking concentrations, and that the network structure could have contributed to it.

Evaluation of extended chain

The formation of the extended chains was confirmed by evaluating the contour length and end-to-end distance of a molecular chain between the crosslinking points. The contour length is the length of one chain via the bonds, and the end-to-end distance $R(\lambda)$ is the Euclidean distance between both chain ends (Fig. 2). Prior to elongation, the relationship between the contour length and $R(\lambda)$ indicated almost no correlation (Fig. 4b, left). In the early stage of elongation, only $R(\lambda)$ increased, indicating that the molecular chains in the network were extended toward the elongated directions without changing the distribution of the contour length. Additionally, both the contour length and end-to-end distance increased at a certain elongation ratio, and these values were almost identical (Fig. 4b, right, solid line). In this bead–spring model, the bond with a harmonic potential did not correspond to a chemical bond but to a spring between beads or segments, thereby permitting a highly stretched state. Therefore, in this study, the completely extended chain is defined as a molecular chain with an end-to-end distance greater than the average contour length before the elongation (Fig. 4b, broken lines), with a more elongated chain than the initial state of the non-Gaussian chain (Fig. 1c).

The characteristics of the extended chains were evaluated based on the density and persistence of an extended chain under deformation. The ratios of the extended chain $p_{\text{extended chain}}$ began to increase at a certain elongation ratio, where the stress reached two to three times the normalized stress at the steady state, and then further increased with the elongation (Figs. 4a and 4c). More importantly, in terms of the crosslinking concentration, the order of the increase in the ratio of the extended chains was consistent with that in the stress–strain curves, indicating the formation of extended chains derived from network connectivity. To confirm whether the extended chain was formed temporarily or permanently, the persistence of the extended chains was analyzed based on the ratio of an extended chain at λ among extended chains at $\lambda + \Delta\lambda$ ($p_{\text{extended chain}}(\lambda, \Delta\lambda)$). The ratio in the extended chain increased significantly when the extended chain started to form (Fig. 4d). A high $\Delta\lambda$ increased the frequency, which was likely due to an increase in the number of extended chains as the elongation ratio increased. Hence, it was suggested that extended chains formed persistently on specific chains in the network.

The orientations and lengths of the bonds were examined to evaluate the characteristics of the extended chains. The order parameter of the bond orientation $S_{\text{d}}(\lambda)$ in the non-extended chain increased with the elongation ratio, whereas that in the extended chains was approximately 0.9 (Fig. 5a), where the order parameter was 1 when the chains were completely aligned toward the elongated direction. The lengths of the bonds $a_{\text{s}}(\lambda)$ in the extended chains were greater than the equilibrium length; subsequently, they increased with elongation (Fig. 5b). For the non-extended chains, the bond lengths rarely changed (Fig. 5b). Hence, the bonds in the extended chains were aligned and

stretched in the elongation direction, whereas those in the non-extended chain were less oriented in the non-stretched state. This suggests that the bonds in the extended chains were relatively forced.

The distributions of the extended and non-extended bond lengths were analyzed to reveal the extended chains in more detail. Prior to the elongation, the length of the bonds $a_s(\lambda)$ almost obeyed a Gaussian distribution (Fig. 5c, $\lambda = 1$). In the case of $c/c^* = 3$ at $\lambda = 4$, where the extended chain began to form, the distribution of extended chains appeared in slightly elongated regions, whereas that of non-extended chains showed a distribution similar to that before elongation (Fig. 5c, $\lambda = 4$). As the elongation proceeded, the distributions of the bond lengths in the extended chains became broader. However, a small shoulder was formed in the high region of $a_s(\lambda)$ (Fig. 5c, $\lambda = 4$, $a_s \sim 1.3$–1.5). To confirm whether the shoulder peak appeared temporally, the lengths of the bonds were plotted at different times. For the non-extended chain, the bond lengths at two different times were not correlated, indicating that the bond lengths fluctuated in one distribution (Fig. 5d). By contrast, two peaks were clearly observed in the bond lengths for the extended chains (Fig. 5d). One peak appeared in the slightly elongated region of the non-extended chains, whereas another appeared in the longer region of these peaks. More stretched bonds can be derived from the highly extended chains. These results indicate that the distribution of the bond lengths in the extended chains was different from that of the non-extended chains, and a slight amount of extremely elongated bonds were significantly forced in the extended chains.

Description of extended chain based on complex network analysis

It is speculated that the network structure may result in the formation of extended chains because the extended chains appeared in specific locations persistently. Previously, we reported that some parameters based on complex network science, such as centrality, are associated with stress[32, 35]. Therefore, the descriptor based on network theory was evaluated to represent the ratio of the extended chains. The closeness centrality is one of the network parameters in complex network science, where node i ($C_{c,i}$) is defined as the inverse of the mean of distance for other nodes[45].

$$C_{c,i} = \frac{N-1}{\sum_j d_{i.j}}, \qquad (2)$$

where d_{ij} denotes the minimum path length between nodes i and j, and N is the number of nodes. In elastomers, the crosslinking points and connected molecular chains are regarded as nodes and links, respectively. Therefore, the closeness centrality, which represents the centrality of the crosslinking point in the network associated with connectivity, was estimated for each crosslinking point. It is noteworthy that these network descriptors were determined prior to elongation.

Figs. 6a–b show the ratio of extended chain as functions of network descriptors $R(\lambda_0)$ and C_c, where $R(\lambda_0)$ is the initial end-to-end distance before elongation. In regard to the initial end-to-end distance between the crosslinking points, linear relationships between the ratio and $R(\lambda_0)$ were observed in each crosslinking concentration (Fig. 6a). This descriptor, however, cannot represent a unified relationship for elastomers prepared using different crosslinking concentrations. The closeness centrality describes the ratio in

a unified manner (Fig. 6b). Therefore, the closeness centrality is a superior network descriptor that enables the ratio of extended chains without elongations to be predicted. These results indicate that the molecular chains located on the crosslinking points in the center of the network tended to transform into extended chains.

Stress concentration in network scale

Although the formation of extended chains has been discussed in one molecular chain to date, stress concentrations are expected to be formed in wider regions. Therefore, the assortativity of the degree of crosslinking points was evaluated for a network with only extended chains regarded as links to determine whether the chains formed independently or adjoiningly (Figs. 2 and 7). In this case, the degree k represents the number of extended chains that the crosslinking points or node possesses. The assortativity coefficient $r(\lambda)$ provides information regarding the similarity of degree for neighbor nodes, where a positive value indicates that similar degrees are present in the neighboring crosslinking points[46]. For comparison, a random network was constructed, where the same number of links as extended chains were randomly assigned in the network (Figs. 7c–d). The values of $r(\lambda)$ in the elastomers appeared as positive values, where the ratio of the extended chain started to increase and then decreased gradually as elongation proceeded (Fig. 8a). Meanwhile, the values of $r(\lambda)$ in the random network were approximately 0, indicating that the randomly located neighbor nodes with $k = 1$ did not increase the coefficient value significantly (Fig. 8b). This suggests that the neighboring crosslinking points connected by an extended chain possessed the same

degrees or number of extended chains. Subsequently, the variation in the degree was analyzed for the elastomer and random network. For the elastomers, the ratios of the crosslinking point with degree k ($p_k(\lambda)$) increased almost similarly for k = 1 and 2. Subsequently, the ratios with k = 2 dominated a wide range of the elongation ratio (Fig. 8c). The ratio in the random network started to increase in the order of the degree, and that of k = 2 did not appear at the beginning of the formation of the extended chain (Fig. 8d). Hence, in the elastomers, crosslinking points with two extended chains were formed preferentially, implying the formation of stress concentration.

To confirm the stress concentration at the network scale, the number of connected components of the extended chains in clusters were analyzed (Fig. 9a). For the elastomer, more than two connected components of extended chains were formed, whereas the connectivity number was almost one in the random network (Fig. 7). These results indicate that adjoiningly connected extended chains appeared preferentially, resulting in a stress concentration in the heterogeneous elastomers. It was speculated that the newly formed extended chain tended to appear next to the extended chains. Ratios of newly formed extended chains that appeared next to the existing extended chains in the elastomers were significantly higher than those in random networks (Fig. 9b). It is noteworthy that the ratio in the initial stage of the formation was much higher than that in later stage, although many other chains were present in the entire network. These results show that the extended chains appeared adjoiningly, and that stress concentration occurred in the network scales, particularly in the initial stage of the formation of extended chains.

DISCUSSION

Significant effort has been devoted to constructing rubber elastic models that consider the heterogeneity in networks[21-29]. The upturn in stress-strain curve is described by non-Gaussian chain statics using the inverse Langevin function[1, 5-7] (Fig. 1). Subsequently, a completely extended chain associated with strain hardening is formed (Figs. 1 and 2). However, the location at which the extended chains form in the network and the manner by which they affect the stress concentration are not completely investigated. It was previously reported that the elongation ratio at the finite chain extensibility in the stress–strain curve was determined by the crosslinking density and number of segments between crosslinking points[47]. In the current elastomers, the cross-linking density, number of segments between crosslinking points, branch number of the network, and primary-loop fractions were almost identical. However, the elongation ratio at the upturn of stresses depended significantly on the crosslinking concentrations or chain connectivity—a phenomenon that could not be explained using an existing rubber elastic model (Fig. 3)[22]. Another perspective is the formation of completely extended chains in homogeneous elastomer. In the diamond network, deviation from the neo-Hookean model was confirmed, whereas almost no completely extended chain appeared up to $\lambda = 10$. This shows that the finite chain extensibility was afforded without a completely extended chain owing to the loss of entropy, where almost no stress concentration occurred in the homogeneous network. Therefore, the manner by which the molecular chain is connected among the crosslinking points in heterogeneous networks

affects the formation of completely extended chains along with the finite extensibility.

Complex network analyses offer several advantages for studying extended chains in detail. In general, the chain connectivity is analyzed by parameters representing network structure or topological defect at the local scale such as number of dangling chains and loops[21-29]. For instance, the fracture of polymer networks with topological defects and several primary loop fractions based on simulations has recently been reported[40-42]. However, the network structure remains at the local polymer chain scale. Complex network science enables the classification of each polymer chain based on the global network structure. Consequently, although the elastomers in this study possessed almost no dangling chains and primary loops, polymer chains with high closeness centrality tended to be extended. Thus, the complex network analysis represents the predictable behavior of each polymer chain as extended chains based on centrality.

Complex network science approaches stress concentration on a mesoscopic scale. Recently, the stress concentration in soft materials with macroscopic networks has been extensively investigated[48-53], where the connectivity can be recognized by the humans' naked eye. However, the difficulty in quantifying molecular networks with complicated structures has prevented the discussion of stress concentration in elastomers. The current approach of using the assortativity coefficient enables the discussion of a wider network or mesoscopic scale, revealing the stress concentration of elastomers based on the relationships between neighboring nodes or cross-linking points. Cross-linking points with two completely extended chains tended to form, suggesting that the formation of extended chains induced that of neighboring extended chains. Although, in

experiments, an aligned or forced polymer chain or strain-induced crystallization has been revealed by several methods, including rheo-optics, nano atomic force microscopy, mechanochemistry, and scattering measurements[31, 54-58], the connectivity of polymer chains is difficult to visualize. Notably, the fatigue of polymeric materials occurs in a hierarchical order. Hence, our approach represents the relationship between the microscopic structure, mesoscopic structure, and macroscopic properties by bridging the gap between the rubber elastic theory and externalism in a more complicated system.

SIMULATION AND ANALYSIS

Coarse-grained molecular dynamics simulations of elastomers

The simulation procedure performed in this study is similar to that used in a previous study[35]. (Readers may refer to the paper to understand the preparation and elongation methods in detail). In this study, the number of crosslinking points was increased from 100 to 512 to discuss the neighboring states. The Kremer–Grest-type bead–spring model with harmonic and Lenard–Jones potentials for bond and interbead interactions, respectively, was utilized in COGNAC of OCTA software. Two complementarily reactive four-arm star polymers (each containing 256 polymers) were assigned to the simulation boxes with periodic boundary conditions and reacted in several concentrations with a 98% conversion at the least. Subsequently, the boxes were reduced to ρ = 0.85, and then uniaxial elongations were performed under the NVT ensemble. Twenty-five trials were performed for each crosslinking concentration.

Evaluation of extended chain

In this study, a completely extended chain is defined as a molecular chain with an end-to-end distance greater than the average contour length before elongation. The end-to-end distance was calculated as the Euclidean distance between crosslinking points connected by a molecular chain in all directions, while considering the periodic boundary. One simulation included approximately 1000 molecular chains from 512 crosslinking points with four branching points, which resulted in approximately 25000 molecular chains per crosslinking concentration. Therefore, the ratio of extended chains was statistically significant. The order parameter of bonds in the extended or non-extended chains, S_d, is defined as follows:

$$S_d = \frac{1}{2}\left(3 < \mathbf{e}_{bond} \cdot \mathbf{e}_{elongation} > -1\right), \quad (3)$$

where $\mathbf{e}_{bond}$ and $\mathbf{e}_{elongation}$ are the unit vectors of the bond and elongated direction, respectively.

Estimation of closeness centrality, assortativity coefficient, and degree

The closeness centrality was evaluated using the igraph package[46] in the R language. The crosslinking points and connected molecular chains were regarded as nodes and links, respectively. The closeness centrality was calculated based on Equation (2) for each crosslinking point. The closeness centrality was defined for each molecular chain by the sum of the values of the connected crosslinking points. In terms of the plot in Fig. 4, approximately 25000 values of the molecular chains were segregated into five

areas based on the closeness centrality or end-to-end distance, and the average values in each segregated area were plotted. Therefore, one plot included information regarding approximately 5000 molecular chains.

The assortativity coefficient and degree of crosslinking points were calculated for the network with only extended chains using igraph[46] in the R language and NetworkX [59] in the Python package, respectively. The random network was constructed by randomly selecting molecular chains in elastomers containing the same number of extended chains, and the assortativity coefficient and degree were obtained in the same manner.

ACKNOWLEDGEMENTS

This work was supported by JSPS Grant-in-Aid for Scientific Research on Innovative Areas "Discrete Geometric Analysis for Materials Design": Grant Number 17H06468, 20H04644, and 20H04640 and for Scientific Research (B): 20H02800. We would like to thank JSOL for their fruitful discussion of the J-OCTA software. The computer resources were supported by the category of General Projects by the Research Institute for Information Technology, Kyushu University, Joint Usage/Research Center for Interdisciplinary Large-scale Information Infrastructures, and the High Performance Computing Infrastructure in Japan (Project ID: jh200016-NAH). This work was supported by JST, CREST Grant Number JPMJCR17J4, Japan.

Reference:

(1) Kuhn, W.; Grun, F. Relations between elastic constants and the strain birefringence of high-elastic substances. *Kolloid Z* **1942**, *101*, 248-271.

(2) Kubo, R. Statistical Theory of Linear Polymers .2. Elasticity of Vulcanized Rubber. *J Phys Soc Jpn* **1947**, *2*, 51-56.

(3) Yoshikawa, Y.; Sakumichi, N.; Chung, U.; Sakai, T. Negative Energy Elasticity in a Rubberlike Gel. *Phys Rev X* **2021**, *11*, 011045.

(4) Doi, M. *Soft matter physics*; Oxford University Press, 2013.

(5) Wang, M. C.; Guth, E. Statistical Theory of Networks of Non-Gaussian Flexible Chains. *J Chem Phys* **1952**, *20*, 1144-1157.

(6) Davidson, J. D.; Goulbourne, N. C. A nonaffine network model for elastomers undergoing finite deformations. *J Mech Phys Solids* **2013**, *61*, 1784-1797.

(7) Morovati, V.; Dargazany, R. Improved approximations of non-Gaussian probability, force, and energy of a single polymer chain. *Phys Rev E* **2019**, *99*, 052502.

(8) Dietrich, J.; Ortmann, R.; Bonart, R. The Influence of Finite Extensibility of the Chains on the Orientation Behavior of a Polymer Network. *Colloid Polym Sci* **1988**, *266*, 299-310.

(9) Kluppel, M. Finite Chain Extensibility and Topological Constraints in Swollen Networks. *Macromolecules* **1994**, *27*, 7179-7184.

(10) Mao, Y.; Warner, M.; Terentjev, E. M.; Ball, R. C. Finite extensibility effects in nematic elastomers. *J Chem Phys* **1998**, *108*, 8743-8748.

(11) Hoffman, G. G. Effects of bond stretching on polymer statistics. *J Phys Chem B* **1999**, *103*, 7167-7174.

(12) Meissner, B. Tensile stress-strain behaviour of rubberlike networks up to break. Theory and experimental comparison. *Polymer* **2000**, *41*, 7827-7841.

(13) Horgan, C. O.; Ogden, R. W.; Saccomandi, G. A theory of stress softening of elastomers based on finite chain extensibility. *P Roy Soc a-Math Phy* **2004**, *460*, 1737-1754.

(14) Miao, B.; Vilgis, T. A.; Poggendorf, S.; Sadowski, G. Effect of Finite Extensibility on the Equilibrium Chain Size. *Macromol Theor Simul* **2010**, *19*, 414-420.

(15) Yaoita, T.; Isaki, T.; Masubuchi, Y.; Watanabe, H.; Ianniruberto, G.; Marrucci, G. Primitive Chain Network Simulation of Elongational Flows of Entangled Linear Chains: Role of Finite Chain Extensibility. *Macromolecules* **2011**, *44*, 9675-9682.
(16) Millereau, P.; Ducrot, E.; Clough, J. M.; Wiseman, M. E.; Brown, H. R.; Sijbesma, R. P.; Creton, C. Mechanics of elastomeric molecular composites. *P Natl Acad Sci USA* **2018**, *115*, 9110-9115.
(17) Brown, H. R. A model of the fracture of double network gels. *Macromolecules* **2007**, *40*, 3815-3818.
(18) Ducrot, E.; Chen, Y. L.; Bulters, M.; Sijbesma, R. P.; Creton, C. Toughening Elastomers with Sacrificial Bonds and Watching Them Break. *Science* **2014**, *344*, 186-189.
(19) Zhao, X. H. Multi-scale multi-mechanism design of tough hydrogels: building dissipation into stretchy networks. *Soft Matter* **2014**, *10*, 672-687.
(20) Bai, R. B.; Yang, J. W.; Suo, Z. G. Fatigue of hydrogels. *Eur J Mech a-Solid* **2019**, *74*, 337-370.
(21) Miller, D. R.; Macosko, C. W. New Derivation of Post Gel Properties of Network Polymers. *Macromolecules* **1976**, *9*, 206-211.
(22) Edwards, S. F.; Vilgis, T. The Effect of Entanglements in Rubber Elasticity. *Polymer* **1986**, *27*, 483-492.
(23) Everaers, R.; Kremer, K. Topological interactions in model polymer networks. *Phys Rev E* **1996**, *53*, R37-R40.
(24) Panyukov, S.; Rabin, Y. Statistical physics of polymer gels. *Phys Rep* **1996**, *269*, 1-131.
(25) Everaers, R. Entanglement effects in defect-free model polymer networks. *New J Phys* **1999**, *1*, 12.
(26) Rubinstein, M.; Panyukov, S. Elasticity of polymer networks. *Macromolecules* **2002**, *35*, 6670-6686.
(27) Shokuhfar, A.; Arab, B. The effect of cross linking density on the mechanical properties and structure of the epoxy polymers: molecular dynamics simulation. *J Mol Model* **2013**, *19*, 3719-3731.
(28) Zhong, M. J.; Wang, R.; Kawamoto, K.; Olsen, B. D.; Johnson, J. A.

Quantifying the impact of molecular defects on polymer network elasticity. *Science* **2016**, *353*, 1264-1268.
(29) Lin, T. S.; Wang, R.; Johnson, J. A.; Olsen, B. D. Revisiting the Elasticity Theory for Real Gaussian Phantom Networks. *Macromolecules* **2019**, *52*, 1685-1694.
(30) Morita, H.; Miyamoto, A.; Kotani, M. Recoverably and destructively deformed domain structures in elongation process of thermoplastic elastomer analyzed by graph theory. *Polymer* **2020**, *188*, 122098.
(31) Danielsen, S. P. O.; Beech, H. K.; Wang, S.; El-Zaatari, B. M.; Wang, X. D.; Sapir, L.; Ouchi, T.; Wang, Z.; Johnson, P. N.; Hu, Y. X.; et al. Molecular Characterization of Polymer Networks. *Chem Rev* **2021**, *121*, 5042-5092.
(32) Amamoto, Y. Quantitative Evaluation of Connectivity in Elastomers for Describing Rubber Elasticity Based on Network Theory. *Nihon Reoroji Gakk* **2022**, *50*, 95-98.
(33) Yao, H. M.; Hsieh, Y. P.; Kong, J.; Hofmann, M. Modelling electrical conduction in nanostructure assemblies through complex networks. *Nat Mater* **2020**, *19*, 745-751.
(34) Amamoto, Y. Data-driven approaches for structure-property relationships in polymer science for prediction and understanding. *Polym J* **2022**, *54*, 957-967.
(35) Amamoto, Y.; Kojio, K.; Takahara, A.; Masubuchi, Y.; Ohnishi, T. Complex Network Representation of the Structure-Mechanical Property Relationships in Elastomers with Heterogeneous Connectivity. *Patterns* **2020**, *1*, 100135.
(36) Davis, D. A.; Hamilton, A.; Yang, J. L.; Cremar, L. D.; Van Gough, D.; Potisek, S. L.; Ong, M. T.; Braun, P. V.; Martínez, T. J.; White, S. R.; et al. Force-induced activation of covalent bonds in mechanoresponsive polymeric materials. *Nature* **2009**, *459*, 68-72.
(37) Imato, K.; Irie, A.; Kosuge, T.; Ohishi, T.; Nishihara, M.; Takahara, A.; Otsuka, H. Mechanophores with a Reversible Radical System and Freezing-Induced Mechanochemistry in Polymer Solutions and Gels. *Angew Chem Int Edit* **2015**, *54*, 6168-6172.
(38) Liu, C.; Morimoto, N.; Jiang, L.; Kawahara, S.; Noritomi, T.; Yokoyama, H.; Mayumi, K.; Ito, K. Tough hydrogels with rapid self-reinforcement. *Science* **2021**,

372, 1078-1081.
(39) Yamakado, T.; Saito, S. Ratiometric Flapping Force Probe That Works in Polymer Gels. *J Am Chem Soc* **2022**, *144*, 2804-2815. DOI: 10.1021/jacs.1c12955.
(40) Lin, S. T.; Zhao, X. H. Fracture of polymer networks with diverse topological defects. *Phys Rev E* **2020**, *102*, 052503.
(41) Arora, A.; Lin, Y.; Olsen, B. D. Coarse-Grained Simulations for Fracture of Polymer Networks: Stress Versus Topological Inhomogeneities. *Macromolecules* **2022**, *55*, 4-14.
(42) Masubuchi, Y.; Yamazaki, R.; Doi, Y.; Uneyama, T.; Sakumichi, N.; Sakai, T. Brownian simulations for tetra-gel-type phantom networks composed of prepolymers with bidisperse arm length. *Soft Matter* **2022**, *18*, 4715-4724.
(43) Sakai, T.; Matsunaga, T.; Yamamoto, Y.; Ito, C.; Yoshida, R.; Suzuki, S.; Sasaki, N.; Shibayama, M.; Chung, U. I. Design and fabrication of a high-strength hydrogel with ideally homogeneous network structure from tetrahedron-like macromonomers. *Macromolecules* **2008**, *41*, 5379-5384.
(44) Akagi, Y.; Katashima, T.; Katsumoto, Y.; Fujii, K.; Matsunaga, T.; Chung, U.; Shibayama, M.; Sakai, T. Examination of the Theories of Rubber Elasticity Using an Ideal Polymer Network. *Macromolecules* **2011**, *44*, 5817-5821.
(45) *R_clseness*. https://igraph.org/r/html/latest/closeness.html.
(46) *R_assortativity*. https://igraph.org/r/doc/assortativity.html.
(47) Fukahori, Y.; Seki, W. Molecular Behavior of Elastomeric Materials under Large Deformation .2. Rheological Model of Polymer Networks. *Polymer* **1992**, *33*, 1058-1068.
(48) Nakagawa, S.; Okumura, K. Crack-tip stress concentration and mesh size in networks. *J Phys Soc Jpn* **2007**, *76*, 114801.
(49) Driscoll, M. M.; Chen, B. G. G.; Beuman, T. H.; Ulrich, S.; Nagel, S. R.; Vitelli, V. The role of rigidity in controlling material failure. *P Natl Acad Sci USA* **2016**, *113*, 10813-10817.
(50) Yamaguchi, T.; Onoue, Y.; Sawae, Y. Topology and Toughening of Sparse Elastic Networks. *Phys Rev Lett* **2020**, *124*, 68002.
(51) Yan, D. J.; Chang, J. H.; Zhang, H.; Liu, J. X.; Song, H. L.; Xue, Z. G.; Zhang, F.; Zhang, Y. H. Soft three-dimensional network materials with rational bio-

mimetic designs. *Nat Commun* **2020**, *11*, 1180.
(52) Liu, J. X.; Yan, D. J.; Zhang, Y. H. Mechanics of unusual soft network materials with rotatable structural nodes. *J Mech Phys Solids* **2021**, *146*, 104210.
(53) Yin, Y. F.; Zhao, Z.; Li, Y. H. Theoretical and experimental research on anisotropic and nonlinear mechanics of periodic network materials. *J Mech Phys Solids* **2021**, *152*, 104458.
(54) Karino, T.; Okumura, Y.; Zhao, C. M.; Kataoka, T.; Ito, K.; Shibayama, M. SANS studies on deformation mechanism of slide-ring gel. *Macromolecules* **2005**, *38*, 6161-6167.
(55) Shibayama, M.; Karino, T.; Miyazaki, S.; Okabe, S.; Takehisa, T.; Haraguchi, K. Small-angle neutron scattering study on uniaxially stretched poly(N-isopropylacrylamide)-clay nanocomposite gels. *Macromolecules* **2005**, *38*, 10772-10781.
(56) Kureha, T.; Minato, H.; Suzuki, D.; Urayama, K.; Shibayama, M. Concentration dependence of the dynamics of microgel suspensions investigated by dynamic light scattering. *Soft Matter* **2019**, *15*, 5390-5399.
(57) Liu, H. N.; Liang, X. B.; Nakajima, K. Direct visualization of a strain-induced dynamic stress network in a SEBS thermoplastic elastomer with in situ AFM nanomechanics. *Jpn J Appl Phys* **2020**, *59*, SN1013.
(58) Nomura, R.; Liang, X. B.; Iwabuki, H.; Aoyama, T.; Ito, M.; Urayama, K.; Nakajima, K. Heterogeneous Viscoelasticity under Uniaxial Elongation of Isoprene Rubber Vulcanizate Investigated by Nanorheological Atomic Force Microscope and Dynamic Mechanical Analysis. *Nihon Reoroji Gakk* **2020**, *48*, 85-90.
(59) *networkx*. https://networkx.org/documentation/stable/reference/algorithms/generated/networkx.algorithms.components.connected_components.html.

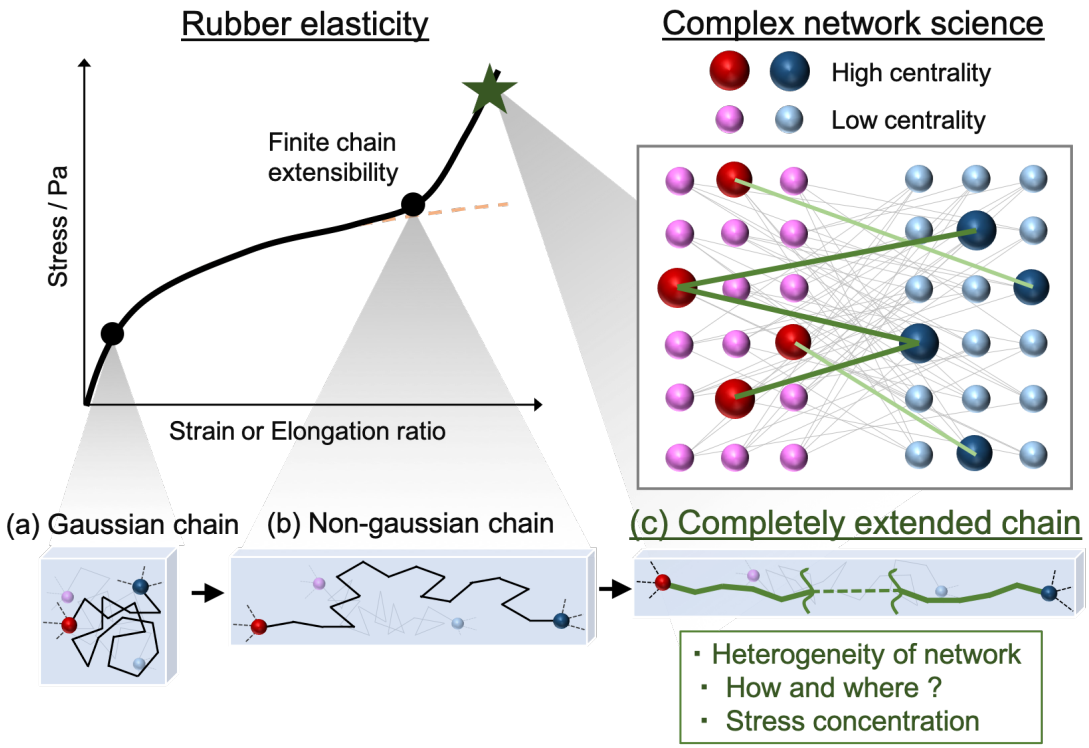

Figure 1. Formation of extended chain in elastomers by finite chain extensibility. Upturn in stress–strain curve of elastomers is typically discussed based on finite chain extensibility. (a) Gaussian chain is assumed in a small deformation region and regarded as a neo-Hookean solid. (b) Upturn in stress is described by non-Gaussian chain due to finite chain extensibility. (c) Progress in deformation of elastomers resulted in formation of completely extended chains. Behaviors of extended chains, particularly those that affect stress concentration, are rarely investigated.

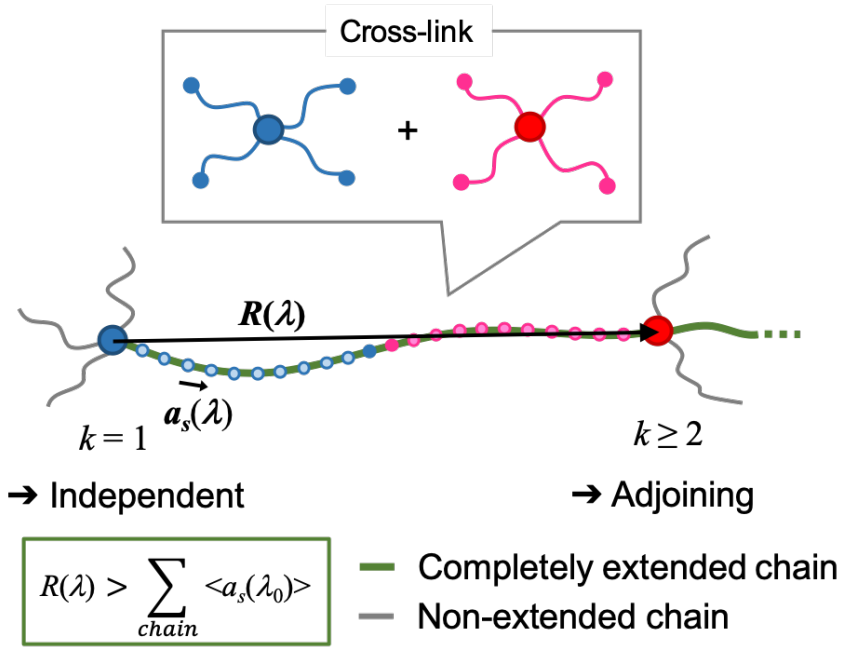

Figure 2. Schematic representation of extended chain. Elastomers were prepared by crosslinking complementary reactive four-arm star polymers. Extended chain was defined as a molecular chain with end-to-end distance exceeding the average contour length before elongation.

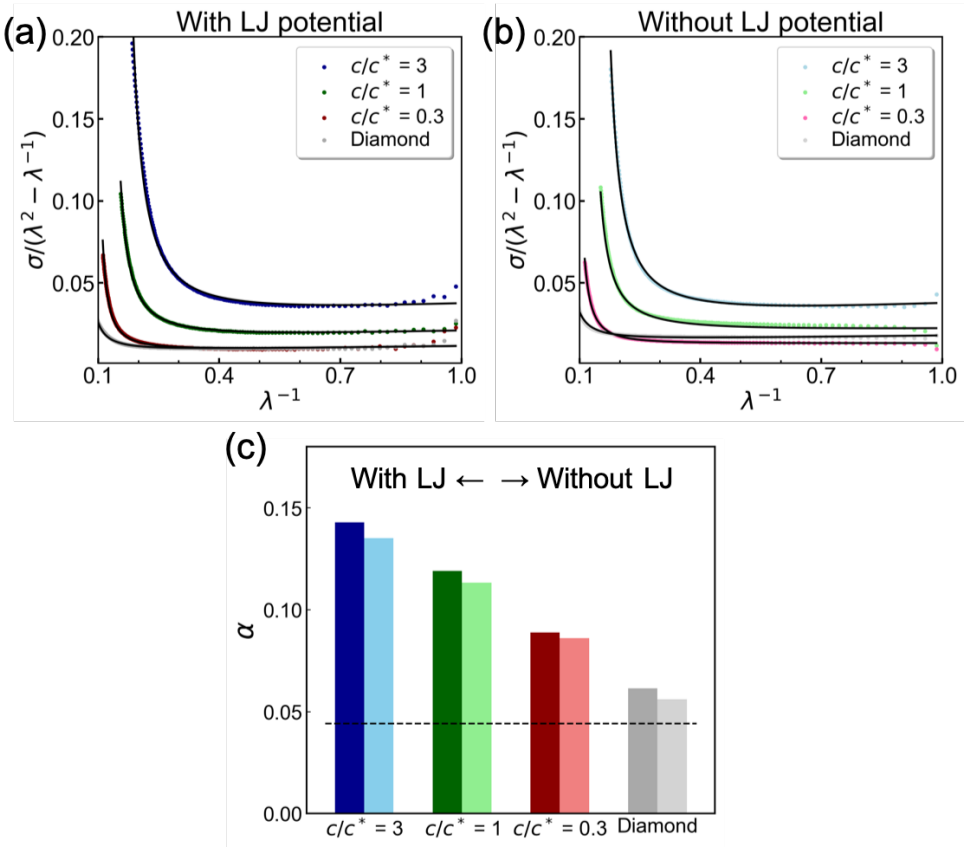

Figure 3. Description of stress–strain curves using rubber elasticity model. Mooney–Rivlin plots of elastomers prepared at c/c^* = 3, 1, and 0.3, and diamond-like elastomer (a) with and (b) without LJ potentials; fitting curves based on theory of rubber elasticity (S. F. Edwards and Th. Vilgis, *Polymer*, 1986). (c) Fitting parameter α for elastomers prepared using different conditions corresponding to finite chain extensibility ($\alpha^{-1} = \lambda_{max}$). Dashed line corresponds to theoretical value calculated using contour length before elongation.

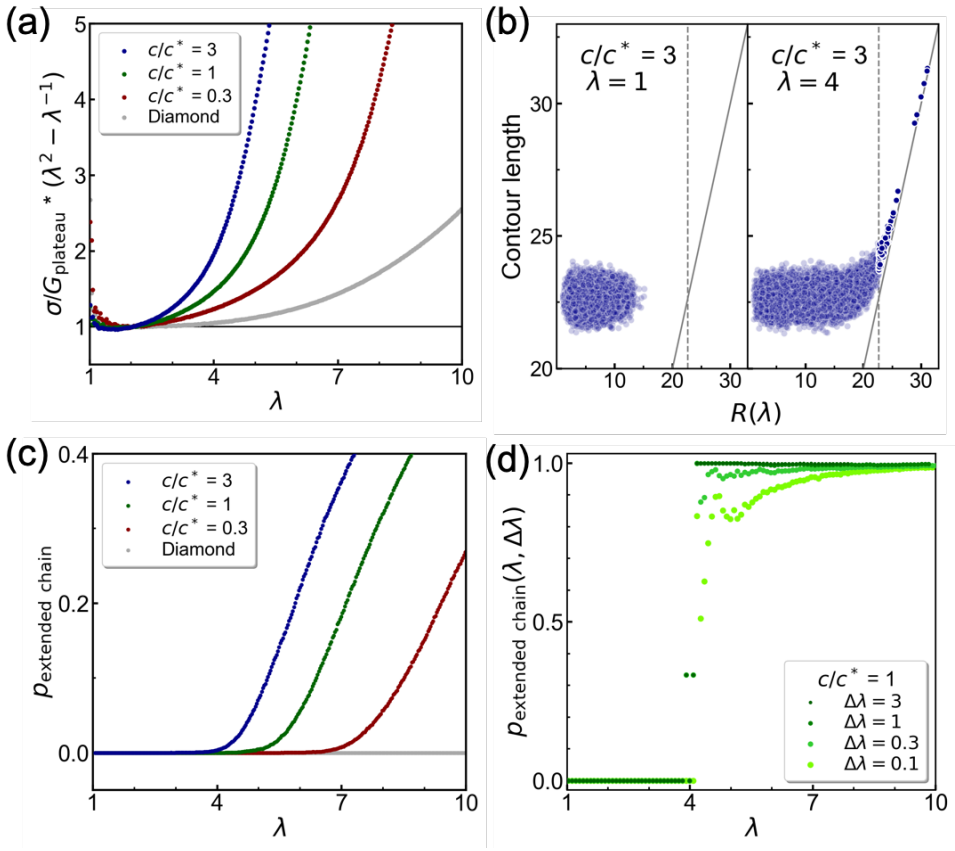

Figure 4. Formation of extended chain under uniaxial elongations. (a) Normalized stresses of crosslinked star polymers prepared at different concentrations using a neo-Hookean model. (b) Contour length as a function of end-to-end distance $R(\lambda)$ at $\lambda = 1$ (left) and 4 (right). (c) Ratio of extended chain ($p_{\text{extended chain}}$) and (d) ratio of extended chain at λ among extended chains at $\lambda + \Delta\lambda$ ($p_{\text{extended chain}}(\lambda, \Delta\lambda)$) under uniaxial elongation. $\Delta\lambda$ corresponds to time difference for comparing persistency of extended chains. Blue, green, and red indicators represent crosslinked star polymers prepared at $c/c^* = 3$, 1, and 0.3, respectively. Gray circle indicates diamond-like network.

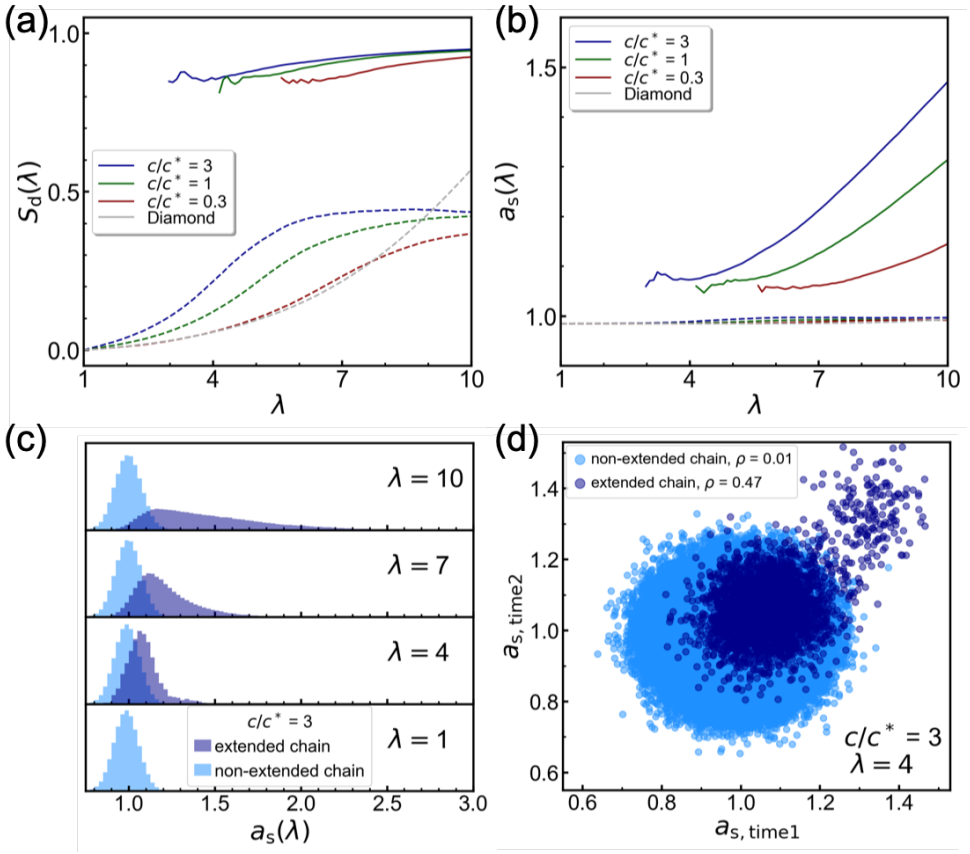

Figure 5. Nature of stretched bonds in extended chains. (a) Order parameter ($S_d(\lambda)$) and (b) length ($a_s(\lambda)$) of bonds in extended and non-extended chains under uniaxial elongation. Solid and broken lines correspond to extended and non-extended chains, respectively. (c) Distribution of bond lengths in extended and non-extended chains at λ = 1, 4, 7, and 10. (d) Correlation of bond lengths at different times. ρ corresponds to correlation coefficient. Blue, green, and red indicators represent crosslinked star polymers prepared at c/c^* = 3, 1, and 0.3, respectively. Gray line indicates diamond-like network.

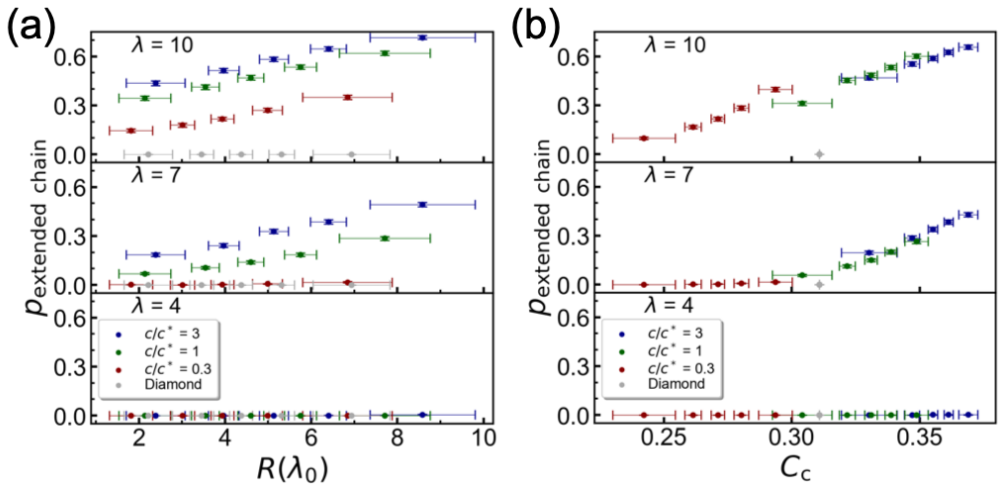

Figure 6. Description of ratio of extended chain based on network descriptors. Ratio of extended chain as a function of (a) initial end-to-end distance $R(\lambda_0)$, (b) closeness centrality C_c, at λ = 4, 7, and 10. Blue, green, and red circles represent crosslinked star polymers prepared at c/c^* = 3, 1, and 0.3, respectively. Error bars in vertical and horizontal axes correspond to 95% confidence intervals of normal distributions and standard deviations, respectively.

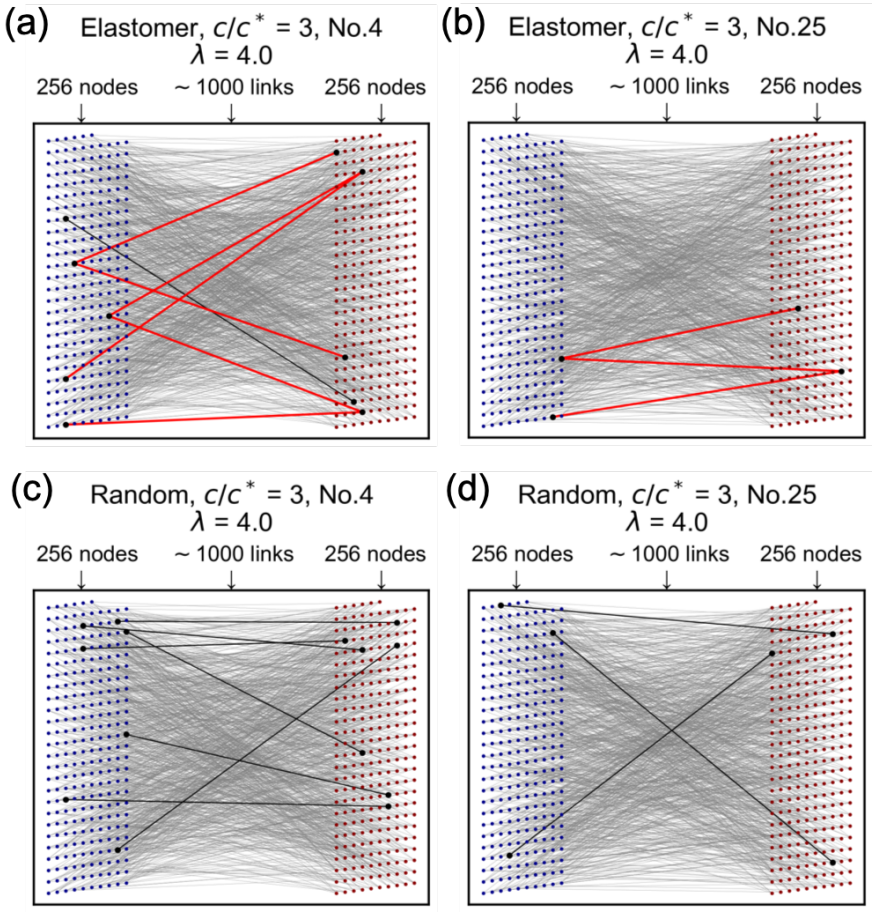

Figure 7. Connectivity of network with merely extended chains. (a-b) Typical connectivity of elastomers with 512 nodes and links of extended chains (black and red lines). Bipartite graphs were obtained because elastomers were prepared via complementary reactions. Links with connectivity number exceeding three of completely extended chains were highlighted by red lines. Thin black and grey lines indicate the extended chains without connecting and non-extended chains, respectively. Two elastomers were selected from 25 simulations. (c-d) Connectivity of random network with 512 nodes and randomly selected links.

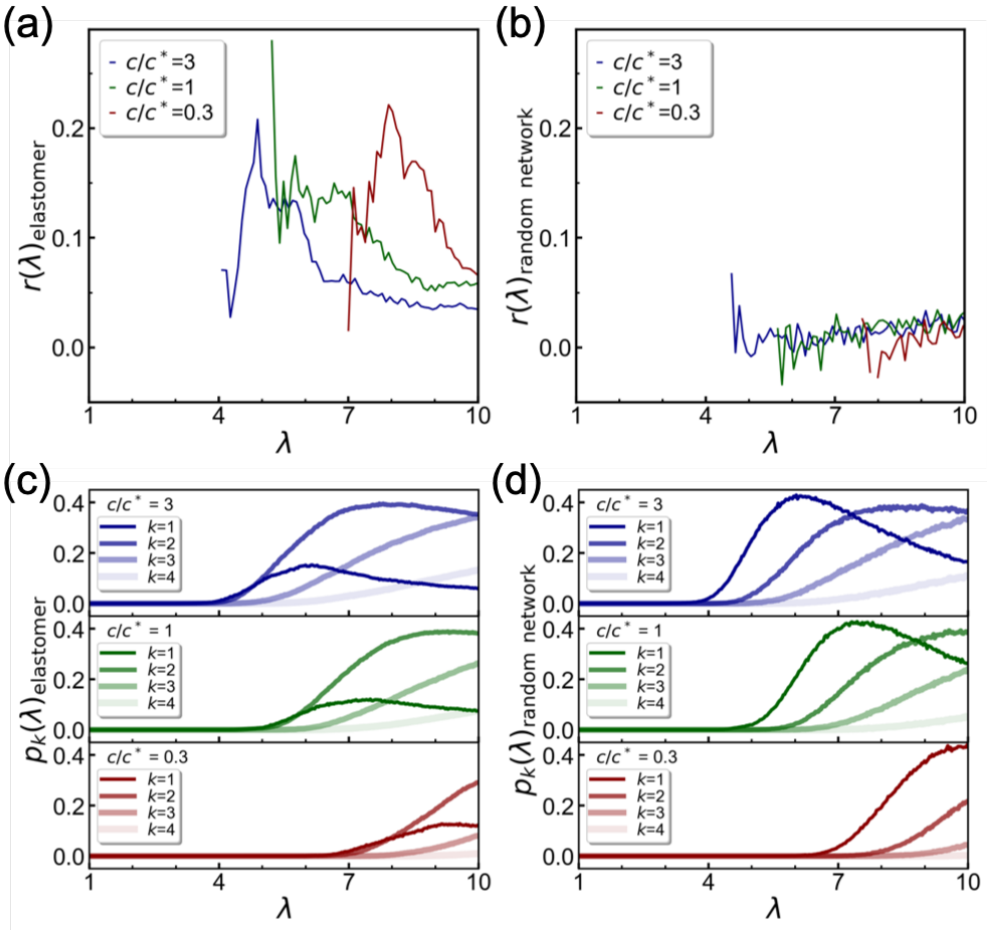

Figure 8. Assortativity coefficient and degree of crosslinking points based on extended chains. Assortativity coefficient of crosslinking points $r(\lambda)$ in (a) elastomer and (b) random network with merely extended chains. Degree of crosslinking points $p_k(\lambda)$ of (c) elastomer and (d) random network with merely extended chains. Degree represents number of extended chains in one crosslinking point. In the random network, extended chains were randomly selected from elastomers with the same number of extended chains. Blue, green, and red circles represent crosslinked star polymers prepared at c/c^* = 3, 1, and 0.3, respectively.

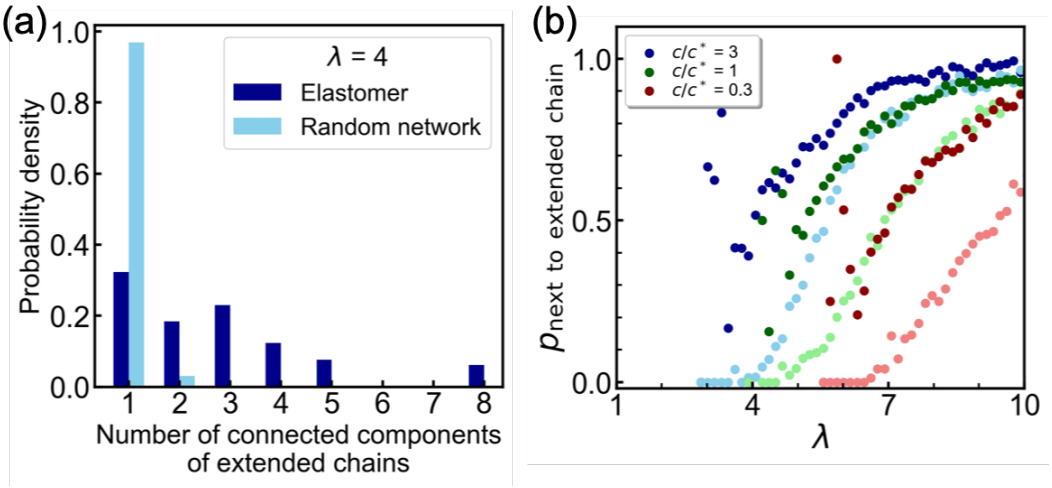

Figure 9. Formation of clusters of extended chains. (a) Histogram of number of connected components of extended chains in elastomer prepared at $c/c^* = 3$ and $\lambda = 4$, and in random network. Random network possesses original connectivity of elastomers and randomly selected links with the same numbers of extended chains. (b) Ratio of newly formed extended chains that appeared next to extended chain among all newly formed extended chains ($p_{\text{next to extended chain}}$) as a function of elongation ratio. Dark blue, dark green, and dark red correspond to extended chains in elastomers prepared at $c/c^* = 3$, 1, and 0.3, respectively. Light color plots represent random networks with the same number of randomly selected links.